Available online at www.sciencedirect.com
SCIENCE DIRECT®
Inorganica Chimica Acta 357 (2004) 2253–2260
Inorganica Chimica Acta
www.elsevier.com/locate/ica

Synthesis, spectroscopy, tandem mass spectrometry, and electrochemistry of the linearly bridged μ-{*trans*-1,4-bis[2-(4-pyridyl)ethenyl]-benzene}-$\{Ru_3O(CH_3COO)_6(py)_2\}_2$ cluster

Sergio H. Toma [a], Sofia Nikolaou [b], Daniela M. Tomazela [c], Marcos N. Eberlin [c], Henrique E. Toma [a,*]

[a] *Instituto de Química, Universidade de São Paulo USP, Caixa Postal 26077, CEP 05513-970 São Paulo, SP, Brazil*
[b] *Departamento de Química da Faculdade de Filosofia, Ciências e Letras de Ribeirão Preto FFCLRP/USP Av. dos Bandeirantes, 3900, 14040-901 Ribeirão Preto, Brazil*
[c] *Instituto de Química, Universidade Estadual de Campinas UNICAMP, 13083-970 Campinas, Brazil*

Received 22 September 2003; accepted 19 November 2003
Available online 24 January 2004

Abstract

The novel polynuclear $[\{Ru_3O(CH_3COO)_6(py)_2\}_2(BPEB)](PF_6)_2$ species containing the linear bridging *trans*-1,4-bis[2-(4-pyridyl)ethenyl]-benzene ligand (BPEB) was synthesized and its structural characterization carried out by means of positive ion electrospray (ESI-MS) and tandem mass (ESI-MS/MS) spectrometry, as well as by ^{1}H NMR spectroscopy. The doubly charged cation $[\{Ru_3O(CH_3COO)_6(py)_2\}_2(BPEB)]^{2+}$ was detected in the ESI-MS mass spectrum as a multiple-component isotopomeric ionic cluster centered at m/z 974, which ion abundance and m/z distribution matched perfectly the isotopic pattern calculated for this multiple isotope Ru_3-containing ion. The tandem mass spectrum of $[\{Ru_3O(CH_3COO)_6(py)_2\}_2(BPEB)]^{2+}$ provided a structural diagnostic dissociation behavior, on the basis of the characteristic charge splitting and sequential ligand loss steps. The cyclic voltammograms of the complex exhibited a quasi-reversible multistep redox behavior, displaying three waves at 1.14, 0.08, and −1.21 V ascribed to the $[Ru_3O]^{2+/1+/0/1-}$ processes and two waves at −1.56 and −1.78 V ascribed to the $BPEB^{0/1-/2-}$ redox processes which are also observed in the free ligand, at −1.48 and 1.61 V, respectively. In spite of the conducting nature of the bridging ligand, the electrochemical and spectroelectrochemical results indicated a weak electronic coupling between the triangular cluster centers.

Keywords: Triruthenium clusters; Conjugated bridging ligand; Tandem mass spectrometry; Nuclear magnetic resonance; Cyclic voltammetry

1. Introduction

Trinuclear complexes of general formula $[M_3O(CH_3COO)_6(L)_3]^n$ (M = transition metal, L = solvent or N-heterocyclic ligands) feature a triangular structure in which the metal ions are held together by μ-oxo and carboxylate bridges [1–3]. In the particular case of triruthenium compounds, the electronic interaction among the ruthenium ions is so strong that the central core $[Ru_3O]^+$ is totally delocalized, and thus behaves as a single metal center [1,4]. From an electrochemical viewpoint, it constitutes an appealing electroactive moiety, since the $[Ru_3O]$ unit displays up to five reversible redox processes from −1.5 to 2.5 V (versus SHE) range and the choice of terminal and bridging ligand modulates its electrochemical behavior [5,6]. Moreover, each monoelectronic process is accompanied by drastic chromatic changes [7,8], providing a suitable combination of electronic stimuli and spectroscopic response.

Here, we report on the synthesis, electrochemistry and spectroscopy a novel dimeric cluster, $[\{Ru_3O(CH_3COO)_6(py)_2\}_2(BPEB)](PF_6)_2$ (Fig. 1) containing a linear bridging ligand (BPEB = *trans*-1,4-bis[2-(4-pyridyl)ethenyl]-benzene). This ligand is particularly interesting due to its strong π-conjugation, suitable for

* Corresponding author. Fax: +55-011-3815-5579.
E-mail address: henetoma@iq.usp.br (H.E. Toma).

0020-1693/$ - see front matter © 2004 Published by Elsevier B.V.
doi:10.1016/j.ica.2003.11.050

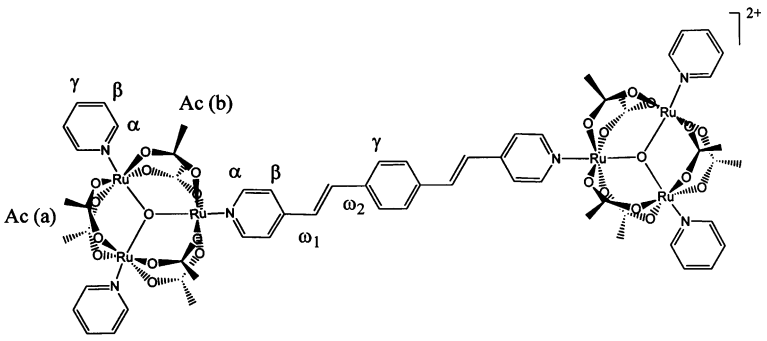

Fig. 1. Structural representation of $[\{Ru_3O(CH_3COO)_6(py)_2\}_2(BPEB)]^{2+}$, showing the labels for ^1H NMR identification.

carrying out electron transport or electronic coupling between remote metal centers [9,10]. Our aim is to assemble a linearly bridged polymetallic species which can be used as low dimension molecular materials, displaying interesting redox and spectral properties.

In addition to the spectroscopic and electrochemical investigation, special attention was given to the application of modern mass spectrometry resources as structural diagnostic tools. In fact, electrospray (ESI) and tandem mass (ESI-MS/MS) spectrometry, which have been mainly (and most successfully) applied to analyze biomolecules [11], are now increasingly being used as structural characterization techniques for inorganic and organometallic compounds [12] transient organometallic intermediates [13–15] and to study intrinsic organometallic catalysis [16]. Taking advantage of the behaved nature of the dimeric cluster system, we have successfully investigated its complete fragmentation pattern by means of positive ion electrospray and tandem mass spectrometry, providing a full interpretation of the dissociation processes involved.

2. Experimental

2.1. Materials

All solvents and reactants were of analytical grade and employed without further purification. The starting $[Ru_3O(CH_3COO)_6(py)_2(MeOH)](PF_6)$ compound was also obtained based on a classical method reported in the literature [17]. *Trans*-1,4-bis[2-(4-pyridyl)ethenyl]-benzene was prepared by the Heck method [18,19] and purified by recrystallization from a hot ethanol-water mixture. *Anal*. Found: C, 83.4; H, 5.8; N, 9.7%. Required for $C_{21}H_{16}N_2$ (MW = 284.36 g mol^{-1}): C, 84.5; H, 5.7; N, 9.6%. Observed $[M+H]^+$: m/z 285.12.

2.2. Synthesis of $[\{Ru_3O(CH_3COO)_6(py)_2\}_2(BPEB)](PF_6)_2$

The $[\{Ru_3O(CH_3COO)_6(py)_2\}_2(BPEB)](PF_6)_2$ complex was prepared by an adaptation of well-established procedures employed by the group [1,2]: *trans*-1,4-bis [2-(4-pyridyl)ethenyl]-benzene (46.7 mg; 0.16 mmol) ligand and three molar equivalents of $[Ru_3O(CH_3COO)_6(py)_2(MeOH)](PF_6)$ (494 mg; 0.48 mmol) were dissolved in a minimum volume of 3:1 MeOH/CH_2Cl_2 (v/v) solution. The mixture was kept stirring in an opened system and eventual solvent evaporation was compensated by adding CH_2Cl_2 to the mixture. After 5 days, ammonium hexafluorophosphate (130 mg; 0.8 mmol) dissolved in a minimum volume of water was added to the resultant deep green solution. The mixture was allowed to precipitate over night, at low temperature. The dark green precipitate was collected on a glass frit by suction filtration, washed with few portions of cold water and diethyl ether and dried in vacuum in the presence of silica-gel. Further purification was performed by gradient elution on a chromatographic column, using neutral alumina (150 mesh) as stationary phase and mixtures of CH_3CN/CH_2Cl_2 as eluent. The relatively non-polar BPEB free ligand eluted first, followed by the unreacted triruthenium complex as the solvent polarity was raised by increasing the amount of CH_3CN added to CH_2Cl_2. When the solvent mixture reached 3:1 CH_3CN/CH_2Cl_2 ratio, a dark green band was eluted and the solvent was removed to dryness in a rotary evaporator. The solid was dried in a vacuum dessicator until constant weight in the presence of anhydrous calcium chloride. *Anal*. Found: C, 34.3; H, 3.5; N, 4.0%. Required for $C_{64}H_{72}N_6O_{26}P_2F_{12}Ru_6$ (MW = 2237.65 g mol^{-1}): C, 34.6; H, 3.2; N, 3.8%. Required for $(C_{64}H_{72}N_6O_{26}^{102}Ru_2^{101}Ru_4)^{+2}$: m/z 973.94. Observed: m/z 974.22.

2.3. Physical measurements

NMR data (1D ^1H and 2D (^1H–^1H) COSY) were recorded on a Varian 300 MHz spectrometer, Model INOVA 1, using $\sim 10^{-2}$ mol dm^{-3} CD_3CN (complex) or $CDCl_3$ (BPEB ligand) solutions. Electrospray mass spectra were recorded on a high resolution Q-Tof (Micromass, UK) mass spectrometer with a quadrupole (Qq) orthogonal time of flight configuration. The sam-

ple, dissolved in pure methanol, was introduced using a syringe pump (Harvard Apparatus, Pump 11) set to 10 μl min^{-1} through an uncoated fused-silica capillary. The ESI spectrum was acquired using a capillary voltage of 3 kV and a cone voltage of 20 V.

Cyclic and differential pulse voltammetry were carried out with a Princeton Applied Research Model 283 potentiostat. A platinum disk electrode was employed for the measurements, using the conventional Luggin capillary arrangement in a 0.100 mol dm^{-3} tetrabutylammonium hexafluorophosphate ($TBAPF_6$) DMF (freshly distilled) solution, with an $Ag/AgNO_3$ (0.010 mol dm^{-3}) reference electrode in acetonitrile containing 0.100 mol dm^{-3} $TBAPF_6$. A platinum wire was used as the auxiliary electrode. Cyclic and differential pulse voltammograms scan rates were 100 and 9 mV/s, respectively. A three-electrode system with a gold minigrid transparent working electrode, mounted inside a conventional quartz cell with restricted internal optical path length (0.025 cm), was used for the spectroelectrochemical measurements. All the $E_{1/2}$ values presented here were converted to SHE by adding 0.503 V to the experimentally obtained values.

3. Results and discussion

3.1. NMR spectroscopy

The ^1H NMR spectrum of the $[\{Ru_3O(CH_3COO)_6(py)_2\}_2(BPEB)](PF_6)_2$ complex (Fig. 2) has been assigned based on the 2D COSY spectra and by comparison with the free ligand and correlated species [20–23]. The results are summarized in Table 1.

The α protons show the largest shifts to higher field in relation to free ligands (Table 1) and the magnitude of the shifts decreases with distance. Smaller shifts are observed for protons β (β_1), γ (γ_1), ω_2, and ω_1. Protons of both, pyridine and bridging ligands, present the same trends of shifts to higher field. This fact can be explained

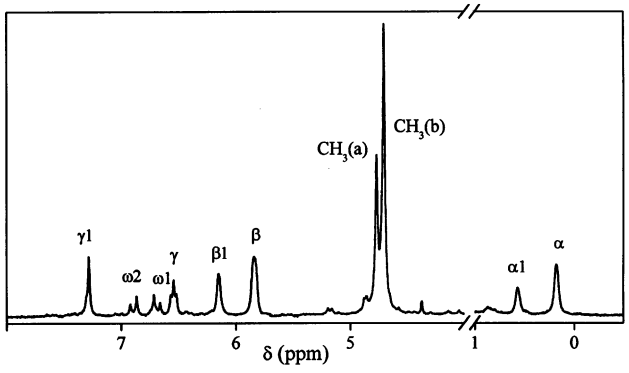

Fig. 2. ^1H NMR spectrum of the $[\{Ru_3O(CH_3COO)_6(py)_2\}_2(BPEB)]^{2+}$ cluster, in CD_3CN (the labels are shown in Fig. 1).

Table 1
^1H chemical shifts (δ/ppm) for the complex $[\{Ru_3O(CH_3COO)_6(py)_2\}_2(BPEB)](PF_6)_2$ and for the free BPEB ligand in CD_3CN and $CDCl_3$, respectively (see labels in Fig. 1)

	Free ligand	$[\{Ru_3O(CH_3COO)_6(py)\}_2(BPEB)](PF_6)_2$
	BPEB[a]	
α_1	8.60 (d, 4H)	0.57 (4H)[b]
β_1	7.39 (d, 4H)	6.15 (4H)[b]
γ_1	7.58 (s, 4H)	7.28 (s, 4H)
ω_1	7.32 (d, $J = 16.2$ Hz, 2H)	6.69 (d, $J = 16.5$ Hz, 2H)
ω_2	7.07 (d, $J = 16.5$ Hz, 2H)	6.89 (d, $J = 16.8$ Hz, 2H)
	Pyridine[c]	
α	8.6	0.18 (8H)[b]
β	7.2	5.83 (8H)[b]
γ	7.6	6.54 (t, 4H)
	Acetate[c]	
(a)	2.1	4.77 (s, 12H)
(b)	2.1	4.70 (s, 24H)

[a] Data collected in this work.
[b] Broad signals due to the paramagnetic anisotropy of the $[Ru_3O]$ moieties.
[c] Data from Sadtler Research Laboratories, Philadelphia, PA, USA.

in terms of the paramagnetic anisotropy of the $[Ru_3O]$ core, which contains one unpaired electron. This effect can operate through two mechanisms (contact and pseudo-contact) [24]; the latter case, also called dipolar mechanism, involves a dipolar interaction through space that decreases with distance. However, it also depends on the orientation of the observed nucleus and the paramagnetic center, making it possible to observe shifts either to high or down field. This explains why the α and α_1 protons show the largest shifts and also the fact that the acetate CH_3 protons are downfield shifted (Table 1), following an opposite trend to that observed for the pyridine protons. Another aspect to be noted is the signal broadening of the protons in α position. Finally, the observed splitting of the signals for the acetate CH_3 groups is consistent with the presence of two magnetically non-equivalent acetate sites; i.e., four *vicinal* and two in opposite position with respect to the bridging ligand.

The spectrum shown in Fig. 2 is consistent with the proposed structure, e.g., there are signals corresponding to only one kind of pyridine ring in the BPEB ligand (labeled as α_1, β_1), confirming the symmetric bridging mode consistent with the dimeric species. It is also worth mentioning that the multiplet corresponding to the BPEB double bonds for both, free and coordinated ligand, displays J values of about 16 Hz, typical of the *trans* conformation [25].

3.2. ESI-MS and MS/MS structure characterization

In Fig. 3, the positive ESI mass spectrum obtained from a $[\{Ru_3O(CH_3COO)_6(py)_2\}_2(BPEB)](PF_6)_2$ methanol solution is shown. In the positive ion mode, ESI

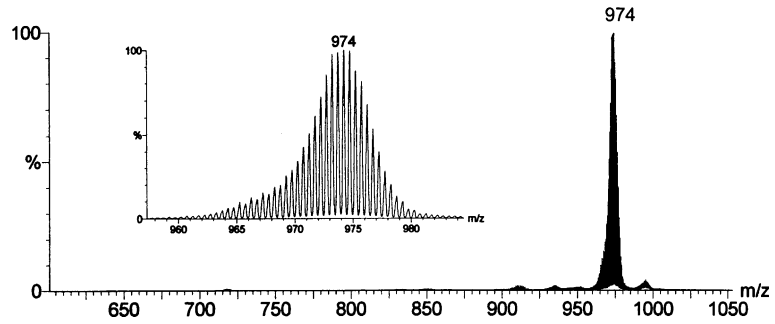

Fig. 3. Positive ion ESI mass spectrum for a methanol solution of $[\{Ru_3O(CH_3COO)_6(py)_2\}_2(BPEB)](PF_6)_2$. The inset shows the ion abundance and the m/z distributions.

detects the cation $[\{Ru_3O(CH_3COO)_6(py)_2\}_2(BPEB)]^{2+}$ as a multiple-component cluster of doubly charged isotopomeric ions centered at m/z 974, with ion abundance and m/z distributions (inset) that match closely the calculated isotopic pattern (not shown). The complex isotopic pattern observed results mainly from the presence of the three multiple isotopic ruthenium atoms [Ru possesses seven isotopes: ^{104}Ru (18.7%), ^{102}Ru (31.6%),^{101}Ru (17.0%), ^{100}Ru (12.6%), ^{99}Ru (12.7%), ^{98}Ru (1.88%), ^{96}Ru (5.52%)].

For refined tandem mass spectrometry structural characterization, the gaseous $[\{Ru_3O(CH_3COO)_6(py)_2\}_2(BPEB)]^{2+}$ ionic cluster centered at m/z 974 was mass-selected for collision-induced dissociation (CID). The product ion mass spectrum (Fig. 4) shows a variety of doubly and singly charged ionic clusters formed by characteristic charge splitting ($M^{+2} \rightarrow F_1^{+1} + F_2^{+1}$) and ligand loss dissociation, as depicted in Scheme 1.

Sequential losses of two neutral pyridines from the parent ion at m/z 974 form two doubly charged ionic clusters centered at m/z 934 and 895. Moreover, the parent ion also dissociates with charge splitting, forming two singly charged ionic clusters centered at m/z 1117 and 833. Further dissociation of the fragment ions at m/z 833 by the loss of one of its pyridine ligand yields the fragments at m/z 754. The species at m/z 1117 fragments further by the loss of either a pyridine or a BPEB ligand, to form the products at m/z 1038 and 833, respectively. Finally, the fragment at m/z 1038 dissociates by loss of the BPEB ligand to form the fragments at m/z 754. Therefore, this characteristic dissociation pattern observed for the gaseous $[\{Ru_3O(CH_3COO)_6(py)_2\}_2(BPEB)]^{2+}$ species, reflects accurately its molecular organization, providing reliable pieces of evidence for its structural elucidation.

3.3. Absorption spectroscopy

The absorption spectra of $[\{Ru_3O(CH_3COO)_6(py)_2\}_2(BPEB)](PF_6)$ can be interpreted by comparing the spectra with the previously reported data for the monomeric $[Ru_3O(CH_3COO)_6\text{-}(py)_2(B)]PF_6$ and dimeric $[\{Ru_3O(CH_3COO)_6(py)_2\}_2\text{-}(B)](PF_6)_2$ (B = bridging ligand such as pyrazine and 4,4′-bipyridine) species reported by Meyer and co-workers [17,26]. The intense band in the UV region can be assigned to the pyridine $\pi \rightarrow \pi^*$ transitions; the near infrared broad band is consistent with the typical IC (intra-cluster) transitions within an energy level manifold generated by the combination of the ruthenium and central oxygen orbitals in the $[Ru_3O(CH_3COO)_6]$ fragment. The intense asymmetric band around 388 nm is expected to be composed by a cluster-to-ligand charge transfer (CLCT) transition (which involves a molecular orbital of the $[Ru_3O]$ center

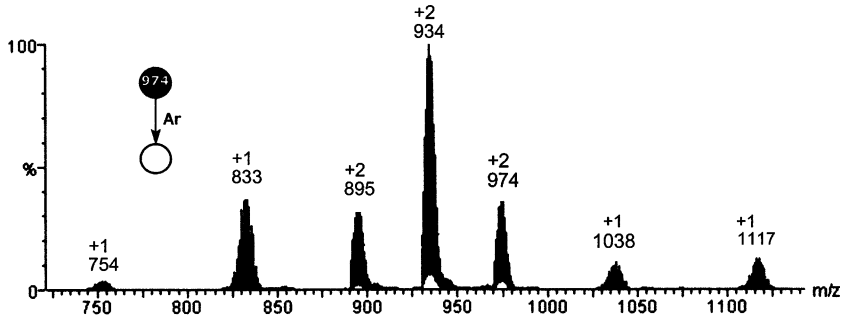

Fig. 4. Tandem product ion mass spectrum for the mass-selected ionic cluster of $[\{Ru_3O(CH_3COO)_6(py)_2\}_2(BPEB)]^{2+}$ centered at m/z 974. The ion shows a structural diagnostic dissociation behavior with characteristic charge splitting and ligand loss dissociation (see Scheme 1). Singly (+1) and doubly (+2) charged ions are labeled.

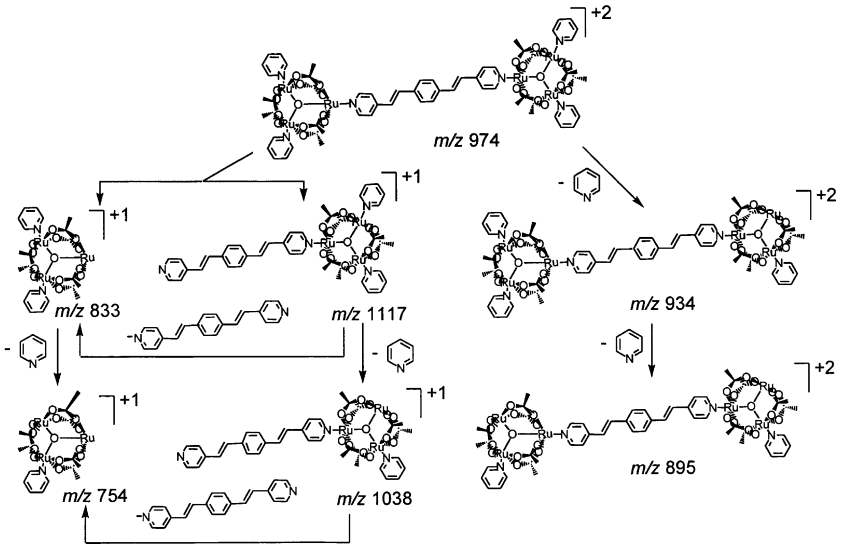

Scheme 1.

and the ligands π^* level), and an intra-ligand (IL) transition of the BPEB. A summary of the spectral data is shown in Table 2.

3.4. Electrochemical and spectroelectrochemical behavior

Cyclic and differential pulse voltammograms of the free BPEB (Fig. 5) consist of two successive, reversible, monoelectronic processes at −1.48 and −1.61 V, which can be ascribed to the sequential reduction of conjugated ligand.

The first reduction of BPEB leads to the decay of the IL band at 356 nm and to the rise of a new band at 646 and 1050 nm, ascribed to $\pi \rightarrow \pi^*$ transitions, similar to those observed in polypyridine radical anion species. In the next reduction step, which yields the $BPEB^{2-}$ anion, both the visible and the near infra-red bands decay, while the $\pi \rightarrow \pi^*$ transition shifts to 315 nm.

Cyclic and differential pulse voltammograms of the $[\{Ru_3O(CH_3COO)_6(py)_2\}_2(BPEB)](PF_6)_2$ dimer (Fig. 7) consist of five sets of waves associated with three successive monoelectronic redox processes of the $[Ru_3O]$ centers and two with the reduction of the BPEB bridging ligand. The corresponding $E_{1/2}$ values are collected in Table 2. There is no evidence of splitting in the redox waves associated with the $[Ru_3O]$ centers, indicating that the electronic interactions through the Ru–BPEB bonds are not strong enough to provide a π-extended system.

According to the spectroelectrochemical results shown in Fig. 8(a), in the 0.99–1.21 V range there is a simultaneous oxidation of the two $[Ru_3O]$ units, from the formal $Ru^{III}Ru^{III}Ru^{III}O$ state to the $Ru^{IV}Ru^{III}$-$Ru^{III}O$ state, leading to a splitting of the intra-cluster band (IC) in the visible region. This process also influences the broad band at 388 nm, composed by the cluster-to-BPEB charge transfer (CLCT) and the

Table 2
Electronic and electrochemical data for the free ligand *trans*-1,4-bis[2-(4-pyridyl)ethenyl]-benzene (BPEB) and for $[\{Ru_3O(CH_3COO)_6(py)_2\}_2$-$(BPEB)](PF_6)_2$ complex

Electronic spectral data	λ_{max} (nm) [ε (mol^{-1} dm^3 cm^{-1})]				
	IL[a]		CLCT[a]	IC[a]	
BPEB	354 (68 178)				
$[\{Ru_3O(CH_3COO)_6(py)_2\}_2(BPEB)]^{2+}$	[b]		388 (48 083)	692 (10 113)	
Electrochemical data	$E_{1/2}$[c] [V] vs. SHE				
	$BPEB^{2-/1-}$	$BPEB^{1-/0}$	$[Ru_3O]^{1-/0}$	$[Ru_3O]^{0/1+}$	$[Ru_3O]^{1+/2+}$
$[\{Ru_3O(CH_3COO)_6(py)_2\}_2(BPEB)]$	−1.78	−1.56	−1.21	0.08	1.14
BPEB	−1.61	−1.48			

[a] IL, intra-ligand; CLCT, cluster to ligand charge transfer; IC, intra-cluster.
[b] Superimposed with the CLCT band.
[c] The reported $E_{1/2}$ are equivalent to the DPV E_p values.

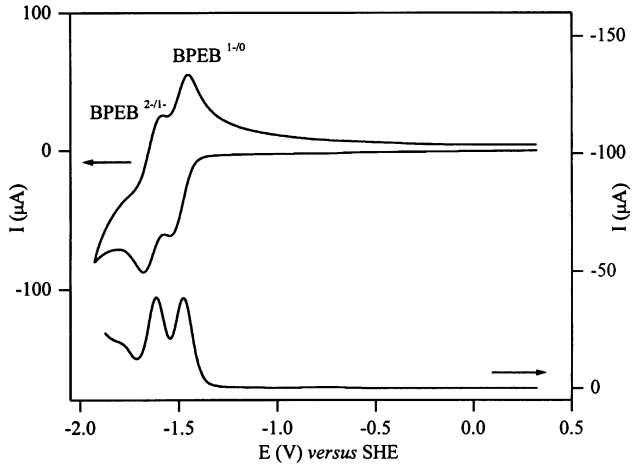

Fig. 5. Cyclic and differential pulse voltammograms of the BPEB free ligand in DMF, 0.1 mol dm^{-3} $TBAPF_6$ solution, at room temperature.

intra-ligand transitions (IL). As the oxidation takes place, it becomes narrower and shifts to 381 nm, due to the decay of the CLCT band, leaving the IL band of the BPEB unchanged.

The first reduction process of the $[Ru_3O]^{1+}$ moieties, shown in Fig. 8(b), in the range from 0.23 to 0.03 V, corresponds to the $Ru^{III}Ru^{III}Ru^{III}O/Ru^{III}Ru^{III}Ru^{II}O$ process, leading to a large bathochromic shift of the IC band from 692 to 926 nm. The addition of one electron in each $[Ru_3O]$ core promotes a general increase in the energy of the occupied electronic levels, being responsible for the red shift of the IC band [1,17]. In agreement with this expectation, the CLCT bands also suffer a bathochromic shift (from 388 to 528 nm). The next electrochemical process is observed in the range from −0.92 to −1.23 V, as shown in Fig. 8(c), corresponding to the $Ru^{III}Ru^{III}Ru^{II}O/Ru^{III}Ru^{II}Ru^{II}O$ reduction. Analogously to the preceding step, it is accompanied by an additional red shift of the IC band to 980 nm, as a consequence of the energy increase in the electronic levels of the $[Ru_3O]$ core. At this point, one can also observe an absorption increase around 500 and 700 nm and the decay of the IL band at 369 nm, which proceeds in the next potential range scanned.

In Fig. 8(d), from −1.41 to −1.57 V range, one can observe the complete decay of the IL band at 369 nm, and the appearance of a broad band centered at 747 nm, which can be ascribed to the $BPEB^{\cdot-}$ absorption, analogous to the free ligand (Fig. 6(a)). It should be noted that as the reduction proceeds, another process involving the cluster centers can be observed from the decay of the IC band at 980 nm, in parallel with the rise of a new absorption band at 512 nm, typical of fully reduced $Ru^{II}Ru^{II}Ru^{II}$ species lacking the central O atom [7,27]. In fact, it is known that in the $Ru^{III}Ru^{III}Ru^{II}O$ species, the central oxygen atom plays an important role in stabilizing the Ru_3O core, by means of a multicentric

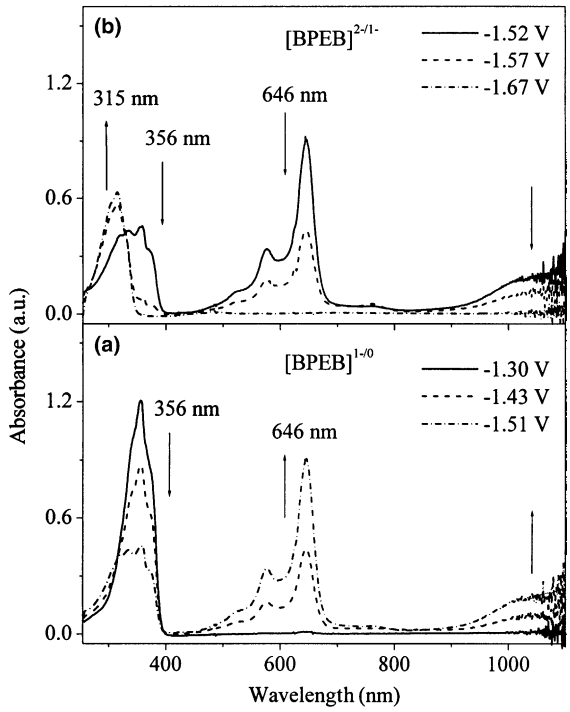

Fig. 6. Spectroelectrochemical behavior of the BPEB bridging ligand in DMF solution; the potential ranges and the assignment of the redox processes are indicated in the figure.

p(π)–d(π) bonding. However, as it is successively reduced, electrons are added to the d_π-orbitals of the Ru(III) ions, such that they become completely filled in the $Ru^{II}Ru^{II}Ru^{II}O$ species. In this case, the interaction between the ruthenium ions and the central oxygen atom is no longer possible, prompting its release from the Ru_3O core [7]. This process can be observed even for the $Ru^{III}Ru^{II}Ru^{II}O$ species. Interestingly, the Ru^{III}-$Ru^{II}Ru^{II}$ species generated in the subsequent chemical

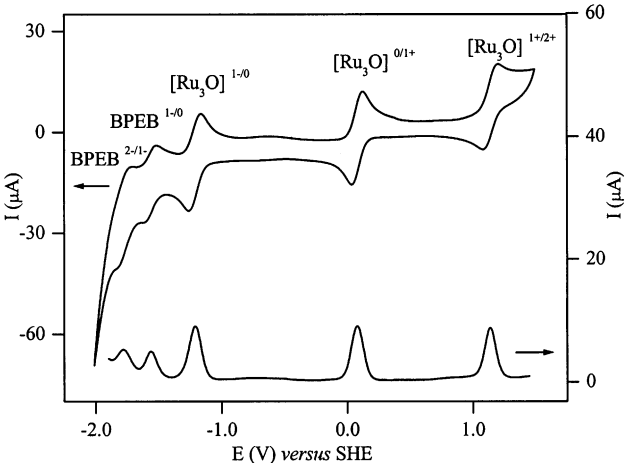

Fig. 7. Cyclic and differential pulse voltammograms of $[\{Ru_3O(CH_3COO)_6(py)_2\}_2(BPEB)](PF_6)_2$ dimer in DMF, 0.1 mol dm^{-3} $TBAPF_6$ solution, at room temperature.

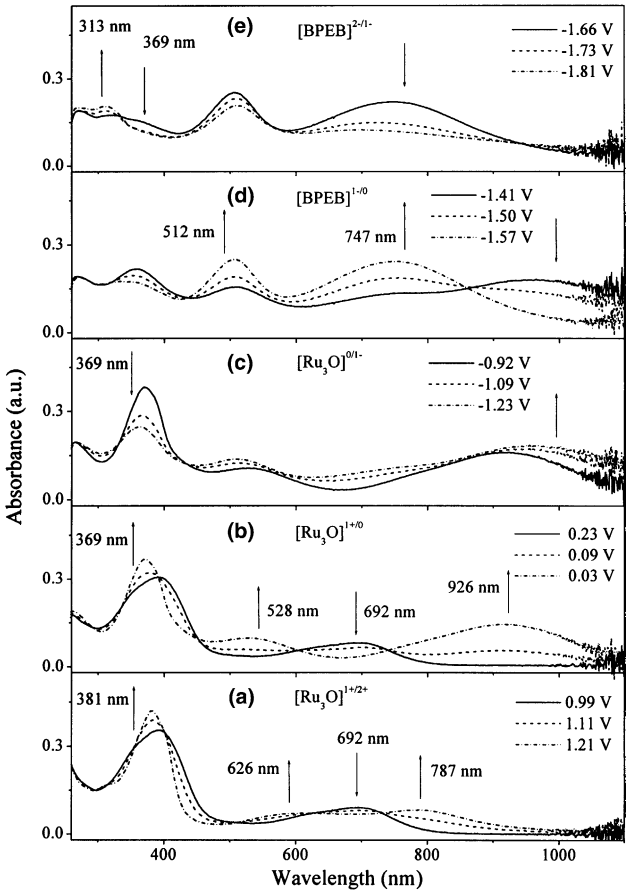

Fig. 8. Spectroelectrochemical behavior of the dimer $[\{Ru_3O(CH_3COO)_6(py)_2\}_2(BPEB)](PF_6)_2$ in DMF solution; the potential ranges and the tentative assignment of the redox processes are indicated in the figure.

reaction exhibits a redox potential dramatically shifted to positive values. In other words, in the time scale of the spectroelectrochemical measurements, the electrochemically generated $Ru^{III}Ru^{II}Ru^{II}O$ species loses the central oxygen atom yielding the intermediate species $Ru^{III}Ru^{II}Ru^{II}$, which is immediately reduced to the $Ru^{II}Ru^{II}Ru^{II}$ form, exhibiting an absorption band at 512 nm (Fig. 8(d), $E < -1.41$ V). This event has not been observed in the cyclic voltammograms, because of the short time scale involved in such measurements. Finally, from −1.66 to −1.81 V range, the bridging ligand is further reduced, as attested by the intensity decrease of the $BPEB^{\bullet-}$ bands centered at 747 and 369 nm (Fig. 8(e)). This behavior is compatible with that observed for the free BPEB ligand (Fig. 6(b)).

4. Conclusions

The $[\{Ru_3O(CH_3COO)_6(py)_2\}_2(BPEB)]^{2+}$ complex constitutes an interesting system where two electronic delocalized cluster units are bridged by a linear conducting ligand. Because of its well-behaved nature, it provides a suitable system for structural investigation combining ^1H NMR spectroscopy with positive ion electrospray (ESI-MS) and tandem mass (ESI-MS/MS) spectrometry. In fact, the doubly charged cation $[\{Ru_3O(CH_3COO)_6(py)_2\}_2(BPEB)]^{2+}$ has been detected in the ESI-MS mass spectrum as a multiple-component isotopomeric ionic cluster centered at m/z 974, which ion abundance and m/z distribution matched closely the isotopic pattern calculated for this multiple isotope Ru_3-containing ion. On the other hand, the tandem mass spectrum of $[\{Ru_3O(CH_3COO)_6(py)_2\}_2(BPEB)]^{2+}$ reveals a well-behaved dissociation pattern, providing structural diagnostic clues on the basis of sequential charge splitting and ligand release steps.

The electrochemical behavior of the binuclear complex in the range from −2.0 to 2.0 V is characterized by two sets of reversible waves (exhibiting 2:1 relative intensities) at 1.14, 0.08 and −1.21 V, ascribed to the $Ru_3O^{2+/1+}$, $Ru_3O^{+/0}$ and $Ru_3O^{0/1-}$ redox couples, and at −1.56 and −1.78 V, ascribed to the $BPEB^{0/1-}$ and $BPEB^{1-/2-}$ redox couples, respectively. The lack of splitting in the voltammetric waves reveals that the two $[Ru_3O]$ units do not form a delocalized type of mixed-valence system. Below −1.2 V, the spectroelectrochemical behavior is influenced by the relatively slow release of the central oxygen atom, leading to the decay of the characteristic intra-cluster bands in the near-infrared region.

Acknowledgements

The authors thank the support from CNPq, FAPESP, RENAMI and the Millennium Institute of Complex Materials.

References

[1] H.E. Toma, K. Araki, A.D.P. Alexiou, S. Nikolaou, S. Dovidauskas, Coord. Chem. Rev. 187 (2001) 219.
[2] A.D.P. Alexiou, S. Dovidauskas, H.E. Toma, Quim. Nova 23 (2000) 785.
[3] T.M. Busleva, S.N. Red'kina, O.V. Rudnitskaya, Russ. J. Coord. Chem. 25 (1999) 3.
[4] R.C. Rocha, H.E. Toma, Quim. Nova 25 (2002) 624.
[5] H.E. Toma, C.J. Cunha, C. Cipriano, Inorg. Chim. Acta 154 (1988) 63.
[6] A.D.P. Alexiou, H.E. Toma, J. Chem. Res. (S) (1993) 464.
[7] H.E. Toma, C. Cipriano, J. Electroanal. Chem. 263 (1989) 313.
[8] H.E. Toma, F. Matsumoto, C. Cipriano, J. Electroanal. Chem. 346 (1993) 261.
[9] M.D. Ward, Chem. Soc. Rev. (1995) 121.
[10] A. Das, J.P. Maher, J.A. McCleverty, J.A.N. Badiola, M.D. Ward, J. Chem. Soc., Dalton Trans. (1993) 681.
[11] R.B. Cole (Ed.), Electrospray Ionization Mass Spectrometry, Wiley, New York, 1997.

[12] R. Colton, A. D'Agostinho, J.C. Traeger, Mass Spectrom. Rev. 14 (1995) 79.
[13] J. Griep-Raming, S. Meyer, T. Bruhn, J.O. Metzger, Angew. Chem. Int. Ed. 41 (2002) 2738.
[14] R. Arakawa, S. Tachiyashiki, T. Matsuo, Anal. Chem. 67 (1995) 4133.
[15] M.N. Eberlin, E. Meurer, L.S. Santos, R.A. Pilli, Org. Lett. 5 (2003) 1391.
[16] D.A. Plattner, Int. J. Mass Spectrom. 207 (2001) 125.
[17] J.A. Baumann, D.J. Salmon, S.T. Wilson, T.J. Meyer, W.E. Hatfield, Inorg. Chem. 17 (1978) 3342.
[18] R.F. Heck, Org. React. 27 (1981) 345.
[19] A.J. Amoroso, A.M.W.C. Thompson, J.P. Maher, J.A. McCleverty, M.D. Ward, Inorg. Chem. 34 (1995) 4828.
[20] H.E. Toma, A.D.P. Alexiou, J. Chem. Res. (S) (1995) 134.
[21] H.E. Toma, A.D.P. Alexiou, S. Nikolaou, S. Dovidauskas, Magn. Reson. Chem. 37 (1999) 322.
[22] A.D.P. Alexiou, H.E. Toma, J. Chem. Res. (S) (1997) 338.
[23] S. Nikolaou, M. Uemi, H.E. Toma, Spectrosc. Lett. 34 (2001) 267.
[24] I. Bertini, C. Luchinat, Coord. Chem. Rev. 150 (1996) 1.
[25] R.M. Silverstein, G.C. Bassler, T.C. Morrill, Spectrometric Identification of Organic Compounds, Wiley, New York, 1991, p. 221.
[26] J.A. Baumann, D.J. Salmon, S.T. Wilson, T.J. Meyer, Inorg. Chem. 18 (1979) 2472.
[27] H.E. Toma, C.J. Cunha, Can. J. Chem. 67 (1989) 1632.